Available online at www.sciencedirect.com
ScienceDirect
Polymer 47 (2006) 8019–8025
polymer
www.elsevier.com/locate/polymer

Preparation of electrospun nanofibers of carbon nanotube/polycaprolactone nanocomposite

Khalid Saeed [a], Soo-Young Park [a,*], Hwa-Jeong Lee [b], Jong-Beom Baek [b], Wan-Soo Huh [c]

[a] Department of Polymer Science, Kyungpook National University, #1370 Sankyuk-dong, Buk-gu, Daegu 702-701, South Korea
[b] School of Chemical Engineering, Chungbuk National University, #14, Gaeshin, Heungduk, Cheongju, Chungbuk 361-763, South Korea
[c] Department of Chemical and Environmental Engineering, Soongsil University, Seoul 156-743, South Korea

Received 28 June 2006; received in revised form 22 August 2006; accepted 3 September 2006
Available online 27 September 2006

Abstract

Multiwalled carbon nanotube/polycaprolactone nanocomposites (MWNT/PCL) were prepared by *in situ* polymerization, whereby functionalized MWNTs (F-MWNTs) and unfunctionalized MWNTs (P-MWNTs) were used as reinforcing materials. The F-MWNTs were functionalized by Friedel–Crafts acylation, which introduced the aromatic amine ($COC_6H_4-NH_2$) groups on the side wall. The F-MWNTs were chemically bonded with the PCL chains in the F-MWNT/PCL, as indicated by the appearance of the amide II group in the FT-IR spectrum. The TGA thermograms showed that the F-MWNT/PCL had better thermal stability than PCL and P-MWNT/PCL. The PCL and the nanocomposite nanofibers were prepared by an electrospinning technique. The nanocomposites that contain more than 2 wt% of MWNTs were not able to be electrospun. The bead of the F-MWNT/PCL nanofiber was formed less than that of the P-MWNT/PCL. The nanocomposite nanofibers showed a relatively broader diameter than the pure PCL nanofibers. The MWNTs were embedded within the nanofibers and were well oriented along the axes of the electrospun nanofibers, as confirmed by transmission electron microscopy.

Keywords: *In situ* polymerization; MWNT; Nanofibers

1. Introduction

Electrospinning was introduced in the 1930s and has recently become an attractive method for the preparation of polymer nanofibers [1] with a submicron diameter. The nanofibers are used for fine filtration [2], scaffold in tissue engineering [3], drug delivery system [4], nanofibrous membrane for high-performance batteries [5] and protective clothing [6]. In the electrospinning process, a high electric field is generated between a polymer solution, which is held in a syringe with a capillary outlet, and a metallic collector. The droplets of the polymer solution from the capillary tip are converted into Taylor cones by an electric field [7]. When the voltage reaches a critical value, the electric forces overcome the surface tension on the droplet and a jet of ultrafine fibers is produced from the tip of the Taylor cone. The advantage of electrospinning is that the polymers can be electrospun in both solution and in a melt state. In the previous researches, polycaprolactone nanofibers were obtained by dissolving them in chloroform [8]. Kim and Lee prepared electrospun nanofibers from the molten state of poly(ethylene terephthalate), poly(ethylene naphthalate) and their blend [9]. Many other polymers such as poly(*p*-phenylene terephthalamide) [10], styrene–butadiene–styrene triblock copolymer [11], polyvinylcarbazole [12], polyurethane [13] and polyaniline–polyethylene oxide blends [14] were also electrospun.

Carbon nanotubes (CNTs) were first reported by Iijima in 1990 and they possess unique mechanical, optical, electrical and thermal conductivity along with chemical stability [15,16]. Due to the unique properties of CNTs, researchers have focused on utilizing these remarkable characteristics for engineering applications such as polymeric composites, hydrogen storage [17], actuators [18], chemical sensors [19]

* Corresponding author. Tel.: +82 53 950 5630; fax: +82 53 950 6623.
E-mail address: psy@knu.ac.kr (S.-Y. Park).

0032-3861/$ - see front matter © 2006 Elsevier Ltd. All rights reserved.
doi:10.1016/j.polymer.2006.09.012

and nanoelectronic devices [20]. The electrical, mechanical and physical properties of the polymeric materials can be improved by the incorporation of a minute amount of CNTs. The dispersion and alignment of CNTs, however, has problems because they are present in the form of bundles and ropes due to Vander wall's forces. Several approaches are used in order to obtain a good dispersion and alignment of the CNTs, such as chemical functionalization [21], wrapping [22] and the synthesis of aligned nanotubes by the deposition of nanotubes onto chemically modified substrate [23]. Recently, the electrospinning technique has also been used for the alignment of CNTs in a polymer matrix [24]. During electrospinning, the alignment of CNTs is expected due to the sink flow and the high extension of the electrospun jet. The alignment of CNTs was also predicted by a mathematical model [25]. The alignment of CNTs in the electrospun nanofibers, however, depends upon the dispersion of CNTs in the polymer solution. The electrospun nanofibers of MWNTs/polyethylene oxide and MWNTs/polyvinyl alcohol [26], MWNTs/epoxy resin [27], MWNTs/polycarbonate [28], and SWNTs/polystyrene and SWNTs/polyurethane [29] composites were also prepared by electrospinning.

In the present study, we functionalized the MWNT by Friedel–Crafts acylation reaction, in which aromatic amines were introduced on the surface of MWNT. The PCL (well known for its unique biocompatibility, degradability [30] and use in medical supplies degradable packing and drug delivery systems) was grafted with aromatic amine functionalized MWNT. In MWNT functionalization, we used polyphosphoric acid and P_2O_5 as drying reagents because they are not only milder and less corrosive than super acid media but also can play the multiple roles such as solvent, Friedel–Crafts catalyst and dehydrating agent [31]. The PCL and multiwalled carbon nanotube/polycaprolactone (MWNT/PCL) composites were also electrospun from a mixture of chloroform and methanol solution. Zeng et al. also grafted PCL with hydroxyl terminated MWNT and focused on the biodegradability of PCL grafted MWNT [32]. In MWNT functionalization, they introduced carboxyl groups on the surface of MWNT (MWNT-COOH) by acid treatment, and then converted MWNT-COOH into acyl chloride by the reaction with thionyl chloride. The acyl chloride functionalized MWNT was converted into hydroxyl functionalized MWNT by the reaction with glycol, and finally, PCL was grafted with hydroxyl terminated MWNT. They observed that the PCL grafted onto CNTs retained the biodegradability of conventional PCL and could be completely biodegraded by pseudomonas (PS) lipase within 4 days. The PS lipase had no effect on the nanotubes, and the nanotubes did little or no biological damage to the PS lipase.

2. Experimental

2.1. Materials

ε-Caprolactone (99% purity) and stannous octoate (95% purity) were purchased from Aldrich and Sigma, respectively, and used as received. Chloroform and methanol (64–66% purity) were purchased from a local company, Ducksan. PCL (average molecular weight 90,000) and the composites were prepared in the author's laboratory [33]. The MWNTs (CVD MWNT 95) were supplied by Iljin Nanotec© and manufactured by thermal chemical vapor deposition [34]. Diameter and length of the studied MWNT (the CVD MWNT 95) were 10–20 nm and 10–50 μm, respectively, and its purity was higher than 97 wt% [34].

2.2. Instrumentation

FT-IR spectra were recorded by using a JASCO FT/IR 620 spectrometer. The samples were spin-coated onto 10-mm diameter KBr pellets. The spectra were derived from 50 coadded interferograms, which were obtained at a resolution of 1 cm^{-1}. The micrographs of the platinum-coated fractured surfaces (broken in the liquid nitrogen) of the nanocomposites and electrospun PCL and the composite nanofibers were taken using a Hitachi S-570 scanning electron microscope (SEM). The TGA thermograms of the composites were obtained in a nitrogen atmosphere, at a heating rate of 20 °C/min between 25 and 900 °C, using a TA4000/Auto DSC 2910 System. Dynamic mechanical analysis (DMA) was performed on the samples (20 (length) × 5 (width) × 0.17 (thickness) mm^3) by using a Diamond Dynamic Mechanical Analyzer (Perkin–Elmer©), in a temperature range between −100 and 60 °C, at a frequency of 1 Hz and a heating rate of 5 °C. The samples for transmission electron microscopy (TEM) were prepared by the direct deposition of the electrospun nanofibers on to the carbon-coated copper grid. The samples were analyzed by using Hitachi M-7600 TEM and the accelerated voltage was 100 kV.

2.3. Functionalization of MWNTs

Scheme 1 shows the side-wall functionalization of MWNTs. Aromatic amines were introduced on the surface of the MWNTs by Friedel–Crafts acylation [31,35]. *p*-Amino benzoic acid, MWNTs and polyphosphoric acid were heated at 120 °C for 3 h, phosphoric penta oxide (P_2O_5) was added, and then the mixture was heated for 12 h. The reacted mixture was cooled and diluted with water, and the precipitates were washed with ammonium chloride. The functionalized MWNTs were soxhlet

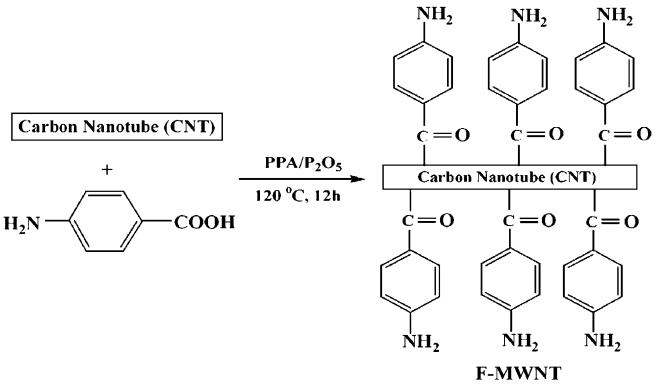

Scheme 1. Side-wall functionalization of MWNT by Friedel–Crafts acylation [31,35].

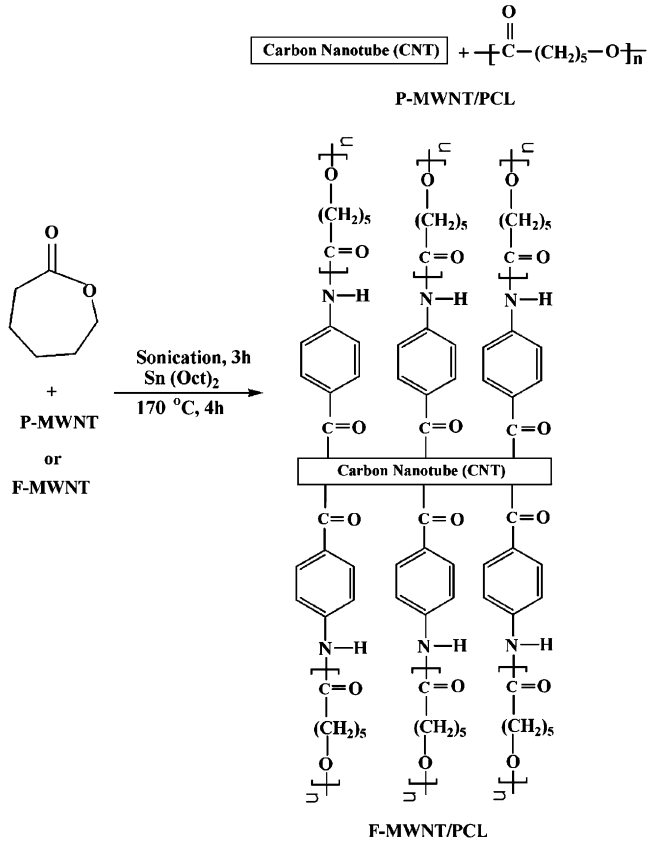

Scheme 2. *In situ* polymerizations of the P-MWNT/PCL and F-MWNT/PCL.

extracted with water and methanol separately for 72 h, respectively, and dried under a reduced pressure at 100 °C for 3 days.

2.4. In situ polymerization of MWNT/PCL nanocomposites

Scheme 2 shows *in situ* polymerizations of the P-MWNT/PCL and F-MWNT/PCL nanocomposites. The synthetic procedure for the P-MWNT/PCL nanocomposites is as follows: a known percentage of P-MWNT and 20 mL of ε-caprolactone were taken in a three-neck round bottom flask. The mixture was sonicated at room temperature for 3 h to produce a homogeneous dispersion of P-MWNTs in ε-caprolactone, and then 0.03 mL of stannous octoate ($Sn(Oct)_2$) was added to the suspension. The flask was then transferred to a preheated oil bath (170 °C) and heated for 4 h with mechanical stirring under a nitrogen atmosphere. The same procedure was used for the F-MWNT/PCL nanocomposites.

2.5. Electrospinning

The solutions of the PCL and MWNT/PCL nanocomposites were prepared by dissolving a 7 wt% sample in a mixture of chloroform and methanol (3:1 ratio) [36]. The MWNT/PCL nanocomposite solutions were sonicated for 1 h in order to obtain a homogeneous dispersion. The same procedure was used for 10 wt% and 15 wt% concentrations.

The prepared PCL solution was added to a 10-mL glass syringe with a needle tip diameter of 0.5 mm. The feeding rate of the polymer solution was 2 mL/h, which was controlled by a syringe pump. The electrospinning voltage (15 kV) was applied to the needle at room temperature and the distance between the needle tip and collector was 11 cm. At a critical voltage, the jet of the polymer solution came out from the needle tip and was collected on the collector. When the solvent evaporated, a non-woven PCL mate was formed. The same experimental conditions were applied for the MWNT/PCL nanocomposites.

3. Results and discussion

Fig. 1 shows the FT-IR spectra of the MWNT, F-MWNT, PCL, P-MWNT/PCL and F-MWNT/PCL. The P-MWNT did

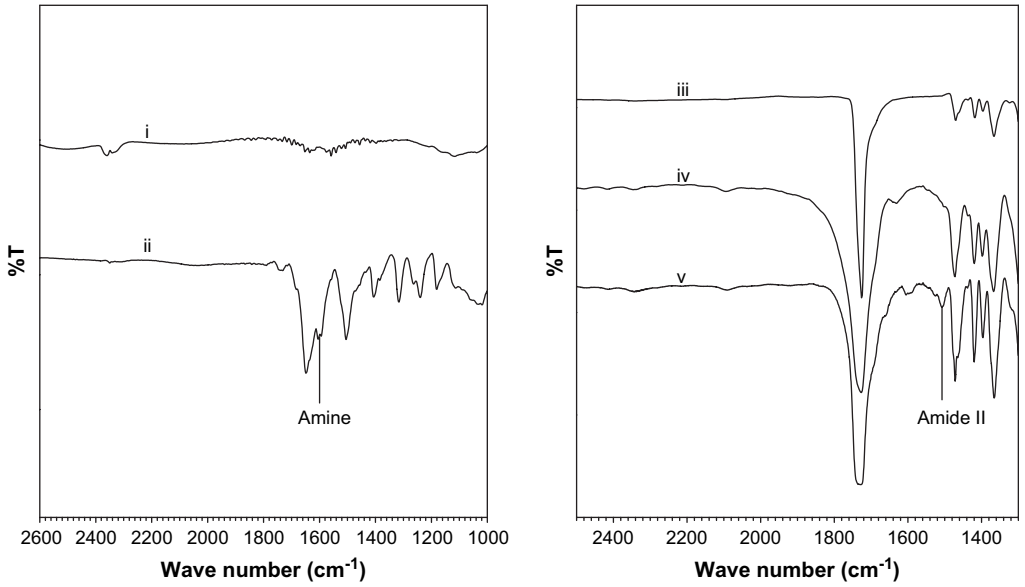

Fig. 1. The FT-IR spectra of (i) MWNT, (ii) F-MWNT, (iii) PCL, (iv) P-MWNT (5 wt%)/PCL and (v) F-MWNT (5 wt%)/PCL.

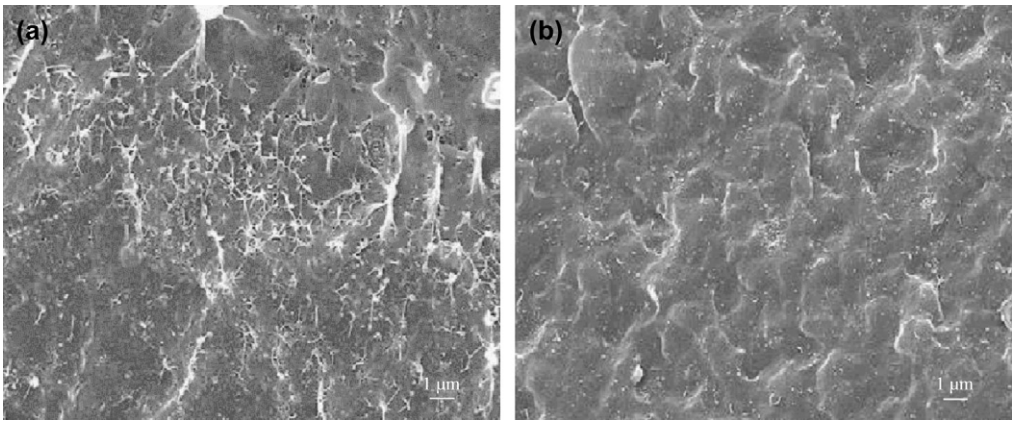

Fig. 2. The SEM images of the fractured surfaces of (a) P-MWNT (5 wt%)/PCL and (b) F-MWNT (5 wt%)/PCL.

not show any particular peak while the F-MWNTs showed a N–H band at 1600 cm^{-1}, indicating that functional groups were introduced [37]. The F-MWNT/PCL showed an amide II group N–H band at 1510 cm^{-1}, which was mainly due to the N–H bending vibration [38]. The appearance of the amide group indicates that the PCL chains were chemically bonded to the side wall of the F-MWNTs.

Fig. 2 shows the SEM microphotographs of the fractured surfaces of the P-MWNT (5 wt%)/PCL and F-MWNT (5 wt%)/PCL. The F-MWNTs in the F-MWNT (5 wt%)/PCL were dispersed well as compared to the P-MWNTs in the P-MWNT (5 wt%)/PCL. The more dispersion of MWNT in the F-MWNT/PCL is due to the chemical modification on the surface of the MWNT, which causes more compatibility with PCL [39,40].

Fig. 3 shows TGA thermograms of the P-MWNT, F-MWNT, PCL, P-MWNT (5 wt%)/PCL and F-MWNT (5 wt%)/PCL. The P-MWNT started to lose weight at 600 °C, while the F-MWNT did at 460 °C. The degradation at 460 °C could be attributed to the loss of aromatic amine in the F-MWNT. The pure PCL and P-MWNT/PCL started to lose weight at 310 °C while the F-MWNT/PCL did at 340 °C, which is 30 °C higher than the pure PCL. The increase of the degradation temperature indicates that the incorporation of F-MWNT into the PCL exerts a thermal stabilizing effect in the composite.

Fig. 4 shows the changes of the storage modulus (E') and tan δ of the PCL, P-MWNT (3 wt%)/PCL and F-MWNT (3 wt%)/PCL, as a function of temperature. The P-MWNT (3 wt%)/PCL and F-MWNT (3 wt%)/PCL showed higher E' than the pure PCL. The temperature at the maximum point in tan δ (representing the glass transition temperature [T_g]) did not change significantly, but the peak was broadened by adding MWNTs in the nanocomposite. It is likely that the major parts of the polymer, which were away from the

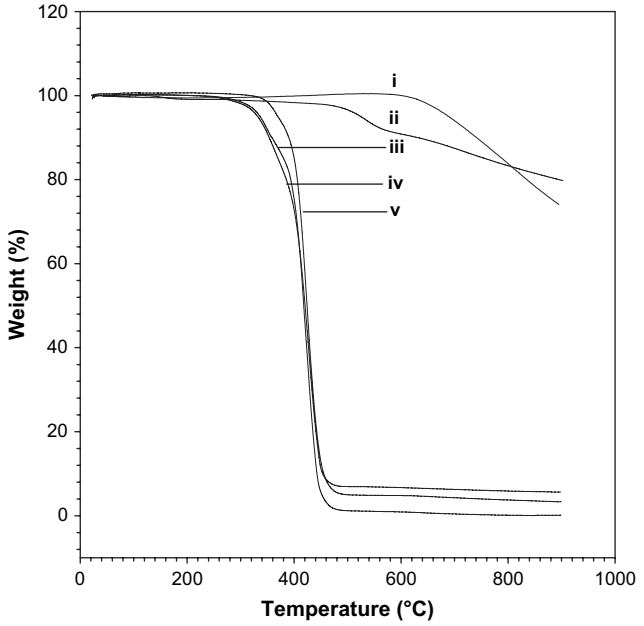

Fig. 3. TGA thermograms of (i) P-MWNTs, (ii) F-MWNTs, (iii) PCL, (iv) 5% P-MWNTs/PCL and (v) 5% F-MWNTs/PCL.

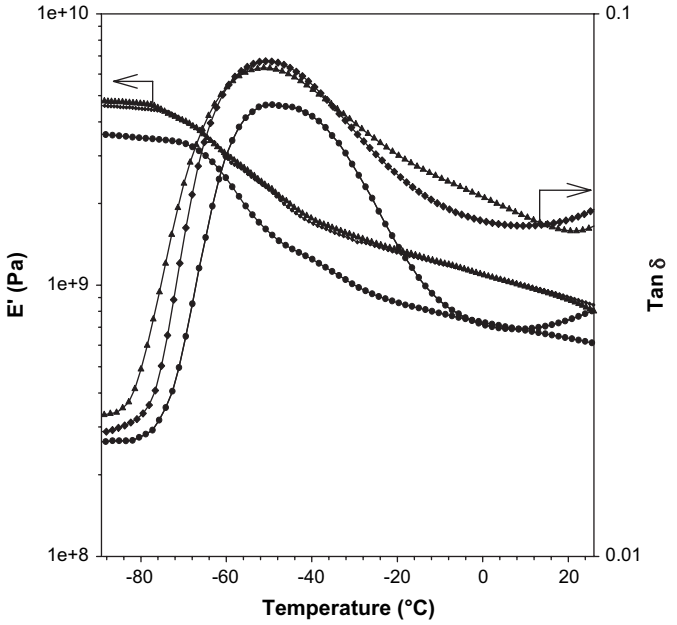

Fig. 4. Storage modulus (E') and tan δ of (●) PCL, (▲) P-MWNTs/PCL and (◆) F-MWNTs/PCL, MWNT 3 wt%.

MWNTs, retained the glass transition temperature of the PCL, while the segments that were close to the MWNTs were less mobile and showed an increase in the glass transition temperature. Similar results of MWNT/PMMA have been reported by Jin et al. [41].

Fig. 5 shows the SEM images of the electrospun PCL nanofibers. The diameters of the electrospun PCL nanofibers were in the range between 100 and 350 ± 50 nm. The nanofiber could not be electrospun when the PCL concentration was lower than 7 wt%; it was only sprayed on a collector. It was also found that the beads were formed during the electrospinning and the number of beads decreased with an increase in the PCL concentration, as shown in Fig. 5. Fong et al. [42] reported that the capillary breaking of the electrospun jets by surface tension led to the formation of the beaded nanofibers. The diameters of the electrospun nanofibers increased with an increase in the concentration of the PCL solution due to an increase in viscosity [43].

Fig. 6 shows the SEM images of the electrospun nanofibers of the F-MWNT/PCL and P-MWNT/PCL nanocomposites. The diameters of the electrospun nanocomposite nanofibers were in the range between 100 and 550 ± 50 nm with a relatively broader size distribution than the pure PCL nanofibers. The bead was formed more with an increase of the amount of MWNTs. The bead of F-MWNT/PCL nanofibers (Fig. 6a–c) formed less than that of the P-MWNT/PCL nanofibers (Fig. 6d–f). The nanocomposites that contained more than 2 wt% of MWNTs were not able to be electrospun although the incorporation of MWNTs increases the shear viscosity of MWNT/PCL, and also electrospinning requires high concentration of the MWNT/PCL solution. The elasticity of the solution was known to decrease by increasing the amount of

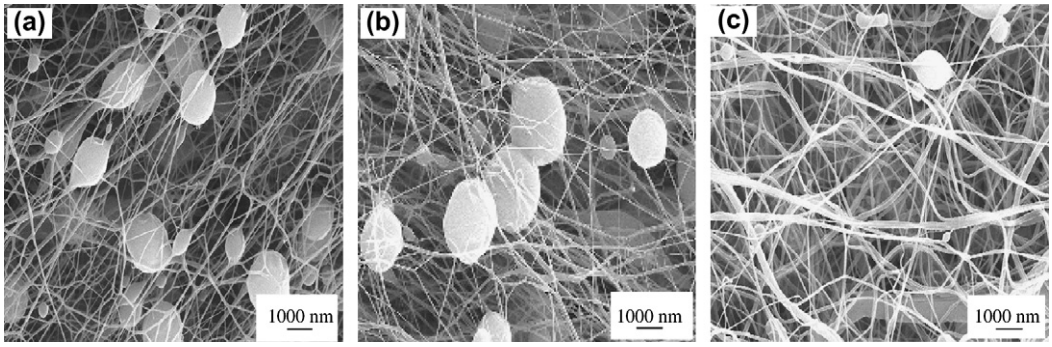

Fig. 5. SEM images of PCL nanofibers made from (a) 7, (b) 10 and (c) 15 wt% PCL solutions.

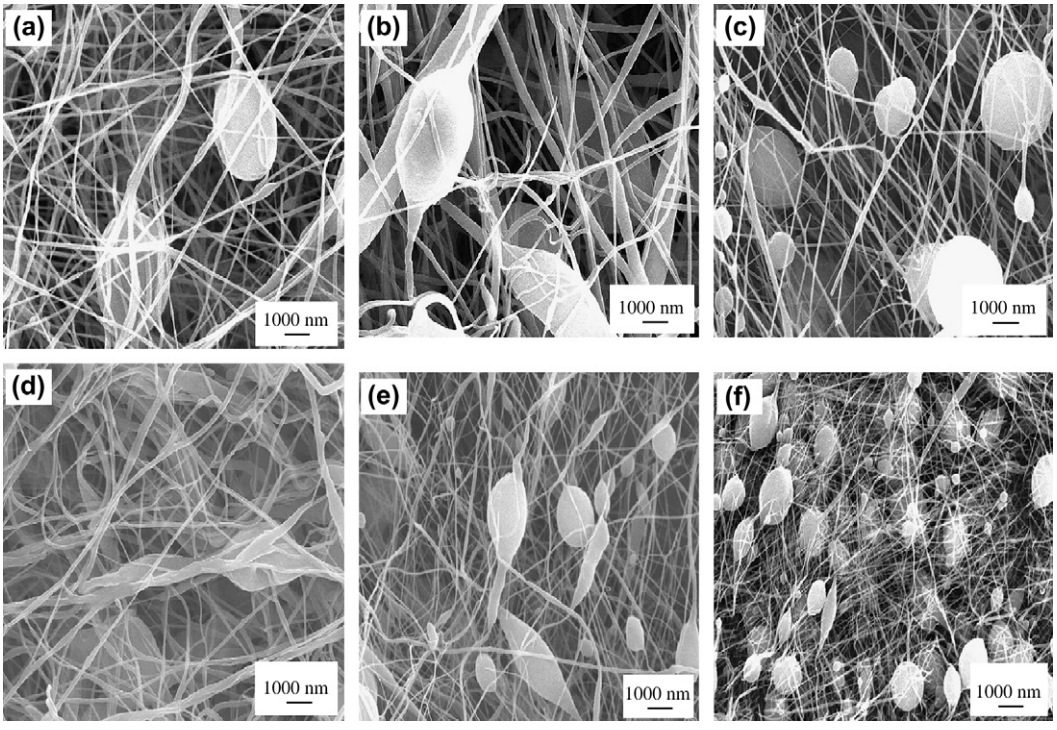

Fig. 6. SEM images of F-MWNT/PCL and P-MWNT/PCL nanofibers made from the 15 wt% solution of the different amounts of the MWNTs of (a) 0.5, (b) 1 and (c) 2 wt% for F-MWNT/PCL and (d) 0.5, (e) 1 and (f) 2 wt% for P-MWNT/PCL.

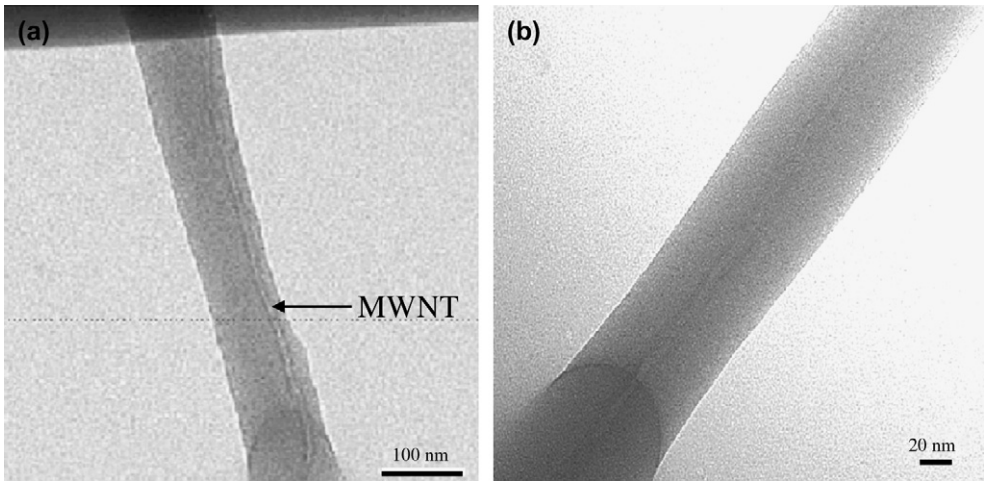

Fig. 7. TEM images of electrospun nanofibers of F-MWNT/PCL nanocomposites.

MWNTs and the reduced elasticity makes electrospinning rather difficult [44].

Fig. 7 shows the TEM images of the electrospun MWNT/PCL nanofibers. The MWNTs were embedded within the fibers and the individual nanotubes (rather than aggregates or bundles) were well dispersed in the nanofibers. Most of MWNTs were well oriented along the axes of the electrospun nanofibers. We found from the TEM study that the MWNTs could be oriented in the polymer matrix by shear force during electrospinning although the orientation of CNT was difficult to be achieved by normal mechanical drawing. The randomly oriented MWNTs in the nanofibers were sometimes observed. They were entangled and knotted, and some even protruded out of the nanofibers. Dror et al. [25] also observed such irregularities in the case of MWNT/PEO.

4. Conclusions

MWNT/PCLs were prepared by *in situ* polymerization, whereby functionalized MWNTs (F-MWNTs) and unfunctionalized MWNTs (P-MWNTs) were used as reinforcing materials. The F-MWNTs were chemically bonded with the PCL chains in F-MWNT/PCL, as indicated by the appearance of amide II group in FT-IR spectrum. The F-MWNT/PCL had better dispersion and thermal stability compared to P-MWNT/PCL. The MWNT/PCL nanofibers were electrospun from the solutions with different concentrations. The beads formation decreased by increasing the concentration of the PCL and the number of beads in the MWNT/PCL composite nanofibers increased by increasing the amounts of MWNT. The MWNTs were embedded within nanofibers and were well oriented along the axes of the nanofibers during electrospinning.

Acknowledgements

This work was supported by Grant No. R08-2003-000-10338-0 from the Basic Research Program of the Korea Science & Engineering Foundation.

References

[1] Demir MM, Yilgor I, Yilgor E, Erman B. Polymer 2002;43:3303–9.
[2] Gibson PW, Schreuder-Gibson HL, Rivin D. AIChE J 1999;45:190–5.
[3] Buchko CJ, Chen LC, Shen Y, Martin DC. Polymer 1999;40:7397–407.
[4] Kenawy E-R, Bowlin GL, Mansfield K, Layman J, Simpson DG, Sanders EH, et al. J Controlled Release 2002;81:57–64.
[5] Mirmohseni A, Oladegaragoze A. Synth Met 2000;114:105–8.
[6] Gibson P, Schreuder-Gibson H, Rivin D. Colloids Surf A Phys-Chem Eng Asp 2001;187–188:469–81.
[7] Taylor GI. Proc R Soc London, Ser A 1969;313:453.
[8] Yoshimoto H, Shin YM, Terai H, Vacanti JP. Biomaterials 2003;24:2077–82.
[9] Kim J-S, Lee DS. Polym J 2000;32:616–8.
[10] Srinivasan G, Reneker DH. Polym Int 1995;36:195–201.
[11] Fong H, Reneker DH. J Polym Sci 1999;B37:3488–93.
[12] Bognetzki M, Frese T, Steinhart M, Greiner A, Windorff JH, Schaper A, et al. Polym Eng Sci 2001;41:982–9.
[13] Cha ID, Kim HK, Lee KH, Jung YC, Cho JW, Chun BC. J Appl Polym Sci 2005;96:460–5.
[14] Kahol PK, Pinto NJ. Synth Met 2004;140:269–72.
[15] Iijima S. Nature 1991;354:56–8.
[16] Wong EW, Sheehan PE, Lieber CM. Science 1997;277:1971–5.
[17] Liu C, Fan YY, Liu M, Cong HT, Cheng HM, Dresselhaus MS. Science 1999;286:1127–9.
[18] Baughman RH, Cui C, Zakhidov AA, Iqbal Z, Barisci JN, Spinks GM, et al. Science 1999;284:1340–4.
[19] Kong J, Franklin NR, Zhou C, Chapline MG, Peng S, Cho K, et al. Science 2002;287:622–5.
[20] Tans SJ, Verschueren ARM, Dekker C. Nature 1998;393:49–52.
[21] Holzinger M, Vostrowsky O, Hirsch A, Hennrich F, Kappes M, Weiss R, et al. Angew Chem Int Ed 2001;40:4002–5.
[22] Hirsch A. Angew Chem Int Ed 2002;41:1853–9.
[23] Schlittler RR, Seo JW, Gimzewski JK, Durkan C, Saifullah MSM, Welland ME. Science 2001;292:1136–9.
[24] Kedem S, Schmidt J, Paz Y, Cohen Y. Langmuir 2005;21:5600–4.
[25] Dror Y, Salalha W, Khalfin RL, Cohen Y, Yarin AL, Zussman E. Langmuir 2003;19:7012–20.
[26] Zhou W, Wu Y, Wei F, Luo G, Qian W. Polymer 2005;46:12689–95.
[27] Allaoui A, Bai S, Cheng HM, Bai JB. Compos Sci Technol 2002;62:1993–8.
[28] Kim G-M, Michler GH, Potschk P. Polymer 2005;46:7346–51.
[29] Sen R, Zhao B, Perea D, Itkis ME, Hu H, Love J, et al. Nano Lett 2004;4:459–64.
[30] Kweona HY, Yoo MK, Park IK, Kim TH, Lee HC, Lee H-S, et al. Biomaterials 2003;24:801–8.

[31] Baek J-B, Park S-Y, Price GE, Lyons CB, Tan LS. Polymer 2005;46: 1543–52.
[32] Zeng H, Goa C, Yan D. Adv Funct Mater 2006;16:812–8.
[33] Saeed K, Park S-Y. Submitted for publication.
[34] <http://www.iljinnanotech.co.kr>.
[35] Baek J-B, Tan LS. Polymer 2003;44:4135–47.
[36] Dalton PD, Klee D, Moller M. Polymer 2005;46:611–4.
[37] Pretsch E, Buhlmann P, Affolter C. Structure determination of organic compounds tables of spectral data. New York, Berlin, Heidelbeg: Springer-Verlag; 2000. p. 269.
[38] Socrates G. Infrared characteristic group frequencies tables and charts. 2nd ed. John Wiley and Sons Ltd.; 1980. p. 99.
[39] Bahr JR, Yang J, Kosynkin DV, Bronikowski MJ, Smally RE, Tour JM. J Am Chem Soc 2001;123:6536–42.
[40] Pompeo F, Resasco DE. Nano Lett 2002;2:369–73.
[41] Jin Z, Pramoda KP, Xu G, Goh SH. Chem Phys Lett 2001;337:43–7.
[42] Fong H, Chun I, Reneker DH. Polymer 1999;40:4585–92.
[43] Ryu YJ, Kim HY, Lee KH, Park HC, Lee DR. Eur Polym J 2003;39:1883–9.
[44] Sung JH, Kim HS, Jin H-J, Choi HJ, Chin I-J. Macromolecules 2004; 37:9899–902.